processes

MDPI

Article

Cost-Effective Processes for Denim Production Wastewater: Dual Criterial Optimization of Techno-Economical Parameters by RSM and Minimization of Energy Consumption of Photo Assisted Fenton Processes via Direct Photovoltaic Solar Panel Integration

Murat Solak

Department of Environmental Engineering, Faculty of Engineering, Düzce University, Konuralp Campus, Düzce 81620, Türkiye; musolak26@gmail.com or muratsolak@duzce.edu.tr

Abstract: Denim production wastewater is an industrial wastewater with a high organic pollutant content. The aim of this study was to improve a cost-effective method via solar panel integration to the photo Fenton process (PFP) and photo electrochemical Fenton process (PEFP) for removing high chemical oxygen demand (COD) from denim production wastewater. To determine process parameter values, the double criterial optimization option was used. The results that maximized the COD removal efficiency and minimized the operating cost of two oxidation processes were determined by response surface methodology (RSM). Optimum operation conditions for the PFP process were 3.18 initial pH, 2.3 g/L Fe^{2+} concentration, and 27 g/L H_2O_2 concentration while they were 3.00 initial pH, 27.06 A/m^2 current density, and 28.16 g/L H_2O_2 concentration for PEFP. At the optimum conditions, COD and the total organic carbon (TOC) removal efficiency of PFP were 85% and 61%, respectively. They were determined as 90% and 73% in PEFP. Carbon oxidation state (COS) and average oxidation state (AOS) parameters were used to obtain the biodegradation capability of organic materials. The biodegradability capability of wastewater was observed as high after the Fenton processes. As a result of the optimization of technical parameters, total operating cost was obtained as USD 14.62/m^3 (USD 4.25/kg$COD_{removed}$) in PFP and USD 13.79/m^3 (USD 3.73/kg$COD_{removed}$) in PEFP. After the integration of the photovoltaic solar panel to the processes, the total operating cost of PFP and PEFP decreased in a ratio of 61% and 64%, respectively.

Keywords: oxidation process; denim production wastewater; dual criterial optimization; operating cost analysis; response surface methodology; photovoltaic solar panel

Citation: Solak, M. Cost-Effective Processes for Denim Production Wastewater: Dual Criterial Optimization of Techno-Economical Parameters by RSM and Minimization of Energy Consumption of Photo Assisted Fenton Processes via Direct Photovoltaic Solar Panel Integration. *Processes* **2023**, *11*, 1903. https://doi.org/10.3390/pr11071903

Academic Editor: Andrea Petrella

Received: 6 February 2023
Revised: 22 February 2023
Accepted: 28 February 2023
Published: 25 June 2023

1. Introduction

Denim is a type of fabric used in jean production. During the production of denim jeans, chemicals that prevent the shrinkage of the jeans, stabilizers, and abrasives are used. Denim jeans, which are washed with chemicals to gain these properties, are then rinsed at least two times. Each denim product goes through at least three washing processes, one of which is chemical washing and two of which are rinsing. Depending on the size of the washing machines, 300 to 500 L of water is used for each wash. This shows how large the amount of water and occurring wastewater is in denim jean production. In short, there is a very high-water requirement in the production of denim jeans, and accordingly, a high amount of wastewater is produced after use. Additionally, this wastewater occurring in the production processes has high concentrations of organic components such as COD, TOC, BOD, and color. COD is an especially important indicator of the degree of pollution in the effluent. COD is determined using a strong chemical oxidant under standard conditions. Biodegradable organic compounds, non-biodegradable compounds, and inorganic oxidizable compounds contribute to COD [1]. Therefore, the removal of COD

from wastewaters has a great importance compared to other parameters. The discharge of textile wastes into water bodies causes toxicity, poor degradability, and the deterioration of environmental quality, such as the reduced self-treatment capacity of receiving waters [2]. Because of these problems, wastewaters occurring in the textile sector have to be treated before discharging them into water bodies. In the treatment of these kind of wastewaters, some methods such as coagulation [3], electrocoagulation [4], and biological [5] and oxidation processes [6] are used. The Fenton process is one of the advanced treatment techniques in which Fe^{2+} and H_2O_2 are used together to form homogeneous $OH^{\cdot}$. In recent years, the usage of Fenton/Fenton-adopted processes has increased in a wide scope [7,8]. While Fenton processes are effective in removing high amounts of organic pollutants in wastewater, they are also effectively used in the treatment of different types of wastewater such as pharmaceutical industry wastewater [9], tannery wastewater [10], dye manufacturing wastewater [11], landfill leachate wastewater [12], coking wastewater [13], etc. Fenton, which is one of the processes used in the treatment of such wastewater, differs from other processes with its various advantages such as treating wastewater with a high organic content with high efficiency, the ease of finding reagents, being effective in a short time [14], relatively low cost and simple operation [15], chemicals of Fenton reagents have low toxicity, and the process works in basic conditions such as at room temperature and atmospheric pressure [16]. To develop the capability of organic material degradation by the Fenton process and to obtain a greater hydroxyl radical formation that offers the usage of a lower concentration of ferrous ion in the Fenton process, UV irradiation was added to the Fenton process, which is called photo-Fenton [17,18]. As a result, it is stated that the organic pollutant removal efficiency of the photo-fenton process is more effective than the classical fenton process [19]. In the photo-Fenton process, the formation of OH occurs by the following reactions (Equations (1) and (2)) [20]:

$$H_2O_2 + h\vartheta \rightarrow OH^{\cdot} + OH^{\cdot} \ (\text{photolysis of hydrogen peroxide}) \quad (1)$$

$$Fe^{3+} + H_2O + h\vartheta \rightarrow Fe^{2+} + OH^{\cdot} + H^{+} \ (\text{photo-Fenton reaction}) \quad (2)$$

The main difference between photo-Fenton and photo-electrochemical Fenton is the additional method of adding Fe^{2+} ions into the wastewater. In the photo-Fenton process, Fe^{2+} ions are added externally, while in the photo-electrochemical Fenton process, Fe^{2+} is added by dissolving it from the Fe electrodes by electrolysis. The electro Fenton process mineralizes almost any organic pollutant in wastewater into carbon dioxide, water, and inorganic species at room temperature and atmospheric pressure. In this respect, the electro-Fenton process can be expressed as cold incineration and allows the effective treatment of wastewater containing toxic, non-biodegradable or persistent substances that cannot be oxidized by conventional processes [16]. To enhance the removal efficiency of Fenton processes, UV is added to the electrochemical Fenton, which is called photo-electrochemical Fenton [21,22]. This process takes place in two ways: (i) the production of hydroxyl radicals by the photo reduction of $Fe(OH)^{2+}$ (Equation (3)) and (ii) the production of Fe^{2+} by the photolysis of Fe^{3+} (Equation (4)):

$$Fe(OH)^{2+} \overset{h\vartheta(k_4)}{\rightarrow} Fe^{2+} + {}^{\cdot}OH \quad (3)$$

$$R(CO_2) - Fe(III) + h\vartheta \rightarrow R({}^{\cdot}CO_2) + Fe(II) \rightarrow {}^{\cdot}R + CO_2 \quad (4)$$

The operating cost of Fenton/electrochemical-Fenton processes varies according to the current density given to the system, the amount of Fenton reagent supplied to the system, and the energy consumption depending on the electrolysis time and the amount of sludge formed. The most important parameter that creates the operating cost in the system is energy consumption. For this reason, renewable energy studies with integrated electrochemical processes have increased in recent years. Solar panel-integrated electrochemical processes give especially good results for minimizing energy consumption and operating

cost [23]. Minimizing energy consumption, which constitutes a very high part of operating costs, contributes to the spread of these processes.

Although there are many articles about Fenton/Fenton-like processes in the literature, studies on the optimization of the techno-economical parameters of the processes are limited. In addition, in the operating cost analysis of Fenton processes, it was determined that the economic parameters of the process such as sludge disposal and chemical costs were not examined in detail. It is thought that this study will make important contributions to the literature in this respect. Despite Fenton/Fenton-adapted processes being effective for organic pollutant removal, the operating costs need to be evaluated in terms of applicability. For this reason, examining the treatment efficiency as well as the operating costs of the treatment techniques provides convenience to the treatment technology selectors in practice. In this study, COD removal, which is the wastewater pollution parameter, and the operating costs of photo-Fenton and electrochemical-Fenton processes were determined. Results that maximize COD removal efficiency and minimize operating costs were developed by the RSM, and after the optimization studies, the effect of photovoltaic solar panel integration into the photo-assisted processes was analyzed.

2. Materials and Methods

2.1. Experimental Flow-Chart and Characterization of Denim Jean Production Wastewater

The experimental chart of the study is given in Figure 1. Denim jean production wastewater was collected from washing machines of the fabric. The wastewater sample used in the experiments was brought to the laboratory under suitable conditions and stored in the refrigerator at about 4 degrees. Afterwards, preliminary experiments were carried out with the samples reaching room temperature, and the ranges of parameters affecting the Fenton processes and COD removal efficiency were determined. The experimental design was created by entering these intervals into the statistical software. The experiments were carried out according to the experimental design. The obtained results were entered into the software, ANOVA analysis was performed, and techno-economic parameters were optimized.

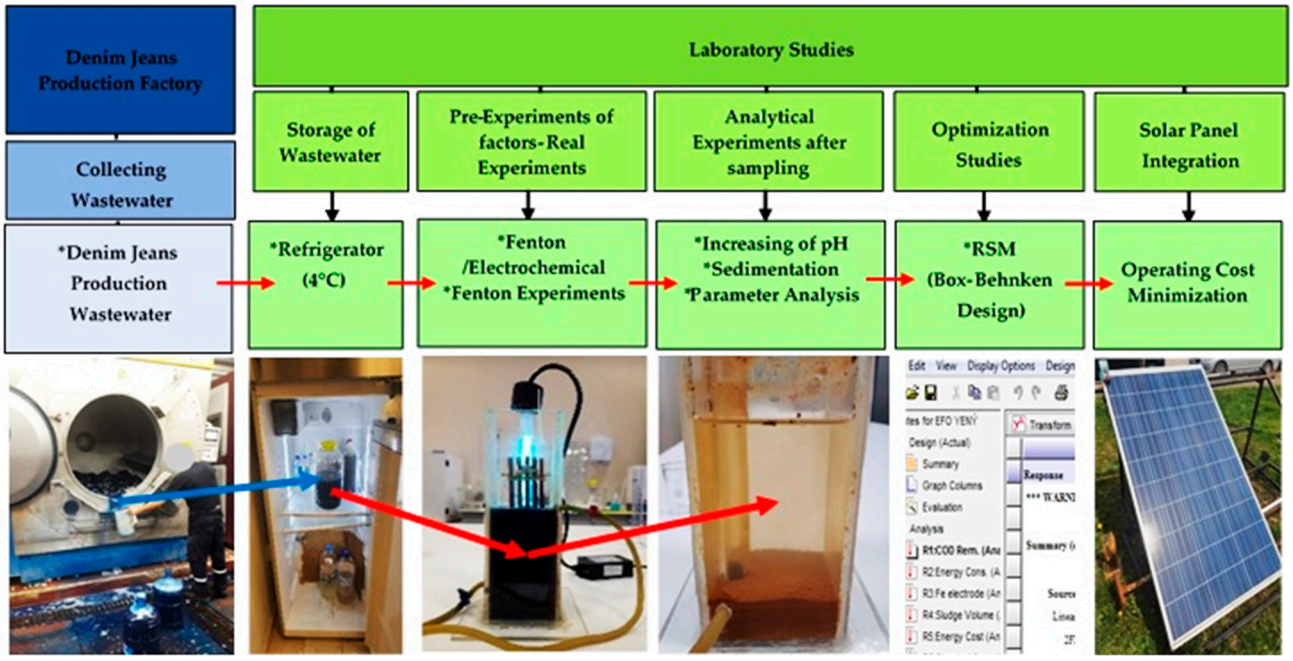

Figure 1. Flowchart of the experimental study.

The characterization of denim jean processing wastewater is given in Table 1. Raw wastewater was supplied from a denim processing factory in Düzce/Türkiye.

Table 1. Raw wastewater characterization.

Parameter	Value/Concentration	Parameter	Value/Concentration
pH	6.82 ± 0.32	TDS	4.89 ± 0.40 g/L
Conductivity	5.16 ± 0.21 mS/cm	Color 460 nm	16 m^{-1}
COD	4100 ± 2000 mg/L	Color 525 nm	35 m^{-1}
TOC	2780 ± 200 mg/L	Color 620 nm	47 m^{-1}
SS	3200 ± 190 mg/L		

2.2. PFP and PEFP Experimental Procedure

In the PFP experiments, 750 mL volume of denim jean production wastewater was added to the reactors (Figure 2a). The power of the UV lamp was 40 W. $FeSO_4 \cdot 7H_2O$ (99.5%) and H_2O_2 (hydrogen peroxide, 50% W/W) were used as a Fenton reagent in the Fenton experiments. Firstly, the pH of the wastewater was adjusted by adding 1 N H_2SO_4. $FeSO_4 \cdot 7H_2O$ was initially added to the pH-adjusted sample, and H_2O_2 was added in the second step. At the same time, after the addition of $FeSO_4 \cdot 7H_2O$ and H_2O_2, the samples were mixed with recirculation by a peristaltic pump (reaction time was optimized as 30 min). When the determined reaction times were completed, the pH of the wastewater sample was increased to 6.5–7.5 by 1 N NaOH solution. Then, the pollutants in the wastewater were allowed to settle for 30 min. The effluent was filtered using 0.45 µm filter papers, and COD, TOC, and other analyses were performed. All experiments were conducted at room temperature, and all the chemicals used in the experiments were of analytical grade.

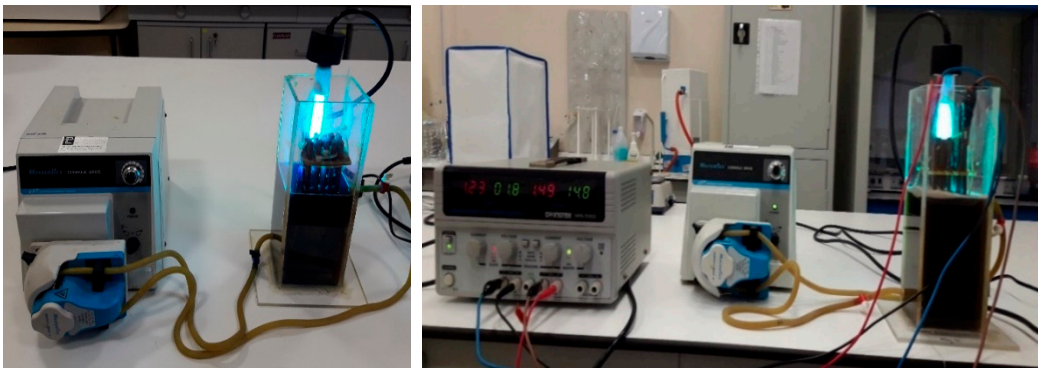

(**a**) (**b**)

Figure 2. Experimental setup: (**a**) PFP; (**b**) PEEP.

In the PEFP experiments, 750 mL volume of denim jean production wastewater was added to the photo-electrochemical Fenton reactor as seen in Figure 2b. Reactor dimensions were 18 cm × 10 cm × 10 cm (H × L × B). The power of the UV lamp was 40 W. The outer surface of the reactor was covered with impermeable material so as not to reduce the effect of the UV light. Ten iron electrodes with dimensions of 1 cm × 20 cm and a thickness of 2 mm were used for the electrochemical Fenton process in the reactor. The samples were mixed with recirculation by a peristaltic pump (reaction time was optimized as 30 min). The pH of the wastewater was adjusted by adding 1 N H_2SO_4. A direct current was applied to the solution, and H_2O_2 was added. The samples were mixed with recirculation by a peristaltic pump (reaction time was optimized as 30 min). When the determined reaction times were completed, the pH of the wastewater sample was increased to 6.5–7.5 by 1 N NaOH solution. Then, the pollutants in the wastewater were allowed to settle for 30 min. The effluent was filtered using 0.45 µm filter papers, and COD, TOC, and other analysis were performed. All experiments were conducted at room temperature.

2.3. Photovoltaic Solar Panel Integration to the Fenton Processes

A photovoltaic solar panel was added to the UV-assisted Fenton processes after the optimization studies. The electrochemical reactor and solar panel integrated into the system are given in Figure 3.

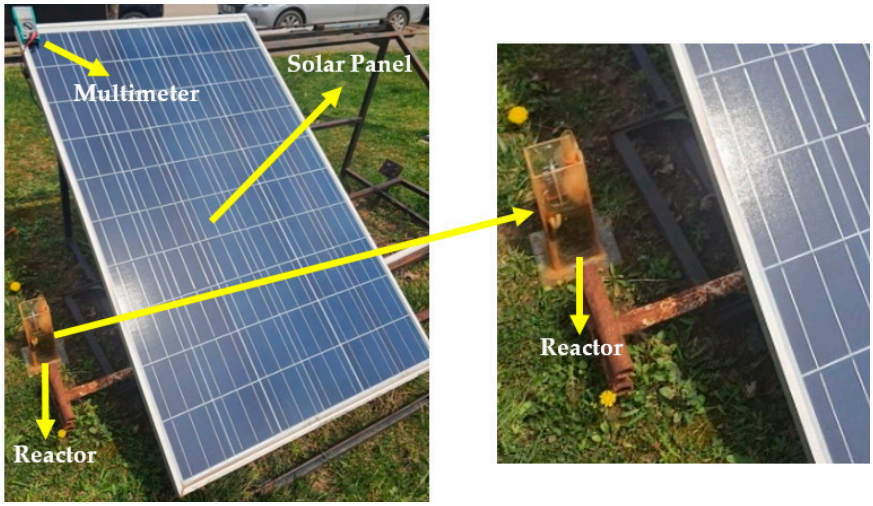

Figure 3. Solar panel integrated EC/EO reactor.

Specifications of solar panel are given in Table 2. Voltage and ampere produced by the solar panel were detected by the multimeter.

Table 2. Technical specifications of the solar panel.

Parameter	Technical Value	Parameter	Technical Value
Solar module type	SPE250	Max system voltage	1000 VDC
Max power (P_{max})	250 W	Dimensions	1001 × 1665 × 42 mm
Max power voltage (Vmp)	30.50 V	Application class	Class A
Max power current (Ipmax)	8.2 A	Weight	18.5 kg
Open circuit voltage (Voc)	37.8 V	Power tolerance up to	+4.9 W
Short circuit voltage (Isc)	8.7 A	Measurement tolerance	±3%

2.4. Analytic Methods

All analytical parameters were measured by the procedures described by the Standard Methods for the Examination of Water and Wastewater (SM) [24] and are given in Table 3.

Table 3. Analytical methods.

Parameter	Method	Method No.	Instrument
COD	Photometric	SM 5220	Hach DR5000 UV-VIS
TOC	High temperature combustion method	SM 5310-B	TOC analyzer with NDIR detector
Suspended Solid	Gravimetric	SM 2540-D	Vacuum filtration unit
Turbidity	Photometric	SM 2130-B	Hach DR5000 UV-VIS
pH	Electrometric	SM 4500-B	Hanna Ins.
Conductivity	Electrometric	SM 2510-B	Hach 7100e
Color	Photometric	EN ISO 7887	Hach DR5000 UV-VIS

2.5. Response Surface Methodology (RSM)

The Box–Behnken Design was used for the optimization of PFP and PEFP for the degradation of COD from the denim jean production wastewater. In PFP, the parameters of pH (X_1), Fe^{2+} concentration (X_2), and H_2O_2 (hydrogen peroxide) concentrations (X_3)

were handled as the variable, while pH (X_1), current density (X_2), and hydrogen peroxide concentration (X_3) were used in the PEFP. This experimental design involved 15 runs, based on a three-level Box–Behnken factorial design. The Design Expert Trial version was used for the statistical analysis of RSM. The parameter ranges and levels are given in Table 4.

Table 4. The ranges and levels for PFP and PEFP.

			PFP			PEFP		
			Levels			Levels		
Coded Variables (X_i)	**Factors**	**Unit**	**Low (−1)**	**Center (0)**	**High (+1)**	**Low (−1)**	**Center (0)**	**High (+1)**
(X_1)	pH	-	3	4.5	6	3	4.5	6
(X_2)	Fe^{2+}/C.D.	g/L-A/m^2	2.3	3.06	3.83	24	48	72
(X_3)	H_2O_2	g/L	23	38.5	54	23	38.5	54

The experimental data were analyzed by the RSM procedure, as seen in Equation (5). In Equation (5), Y is the response (COD removal efficiency (%)) or total operating cost (USD/m^3); $\beta_0\beta_i$ $(i = 1,2,3)$, $\beta_{ij}(i = 1,2,3; j = 1,2,3)$ are the model coefficients; X_i and X_j are the coded independent variables.

$$Y = \beta_0 + \sum_{i=1}^{k} \beta_i X_i + \sum_{i=1}^{k} \beta_{ii} X_i^2 + \sum_{i=1}^{k} \sum_{i=1}^{k} \beta_{ij} X_i X_j + \varepsilon \quad (5)$$

2.6. Equations

Current density is an important parameter in electrochemical wastewater treatment techniques. Current density was calculated by Equation (6):

$$J = I/A \quad (6)$$

In the equation, J is current density (A/m^2), I is current (A), and A is active anode surface area (m^2 or cm^2).

To calculate the COD removal efficiency of Fenton processes from denim jean production wastewater, Equation (7) was used:

$$E_{COD}(\%) = \left(1 - \frac{C_t}{C_0}\right) \times 100 \quad (7)$$

E is the removal efficiency of COD, C_0 is the initial concentration of COD, and C_t is the final concentration of COD.

To determine the energy consumption of the electrochemical systems, Equation (8) was used [25]:

$$E\left(\frac{kWh}{m^3}\right) = -\frac{1}{\forall} \int_0^I VA\, dt \quad (8)$$

In the equation, E is energy consumption, (Wh/m^3), V is voltage (V), A is current (A), t is electrolysis time (hour), $\forall$ is volume (lt or m^3).

The unit prices used in operating cost calculations are shown in Table 5.

Table 5. Unit prices of chemicals, electrodes, and electricity used in the calculations.

Parameter	Unit Price	Parameter	Unit Price
a-Energy	USD 0.22/m^3	e-NaOH	USD 1.74/m^3
b-Fe Electrode	USD 1.00/kg	f-H_2SO_4	USD 1.53/m^3
c-$FeSO_4 \cdot 7H_2O$	USD 1.18/kg	g-Sludge Disposal	USD 0.19/kg
d-H_2O_2	USD 1.76/m^3		

The total operating cost of PFP consists of chemicals used before and after oxidation reactions and energy and sludge disposal costs (Equation (9)).

The abbreviations used in the equations are as follows.

OC_{PFP} Operating cost of PFP (USD/m^3);
OC_{PEFP} Operating cost of PEFP (USD/m^3);
E_{UV} Energy consumption of UV lamp (kWh/m^3);
E_{DC} Energy consumption of DC power supply (kWh/m^3);
E_{PP} Energy consumption of peristaltic pump (kWh/m^3);
C_{FeSO_4} Consumption of $FeSO_4$ (kg/m^3);
$C_{H_2O_2}$ Consumption of H_2O_2 (m^3/m^3);
C_{NaOH} Consumption of NaOH (kg/m^3);
$C_{H_2SO_4}$ Consumption of H_2SO_4 (kg/m^3);
$C_{Fe\ el.}$ Consumption of Fe electrode (kg/m^3);
V_{sludge} Sludge volume (kg/m^3).

$$OC_{PFP} = a \times E_{UV} + a \times E_{PP} + c \times C_{FeSO_4} + d \times C_{H_2O_2} + e \times C_{NaOH} + f \times C_{H_2SO_4} + g \times D_{sludge} \quad (9)$$

For PEFP, the operating cost consisted of chemical, electrode, energy consumption, and sludge disposal cost (Equation (10)).

$$OC_{PEFP} = a \times E_{DC} + a \times E_{UV} + a \times E_{PP} + b \times C_{Fe\ Electrode} + d \times C_{H_2O_2} + e \times C_{NaOH} + f \times C_{H_2SO_4} + g \times V_{sludge} \quad (10)$$

3. Results and Discussion

3.1. Statistical Analysis of COD Removal Efficiency of PFP and PEFP

According to the Box–Behnken Design developed in the RSM tool of Design Expert Software, PFP and PEFP processes were optimized for maximizing COD removal efficiency and minimizing total operating cost.

To determine the significance of the model and the effects of the parameters, DF (degrees of freedom of variance source), SS (sum of squares), MS (mean of squares), F values (F-value of variance source), and *p* values (probability of error to be significant) were obtained from the ANOVA analysis. Other statistical parameters such as R^2 (coefficient of regression), adjusted R^2, predicted R^2, PRESS (predicted residual error sum of squares), and C.V. (coefficient of variation) values are given in Table 6.

R^2, adjusted R^2, and predicted R^2 were checked to determine the adequacy of the models. The quadratic model had a high signal, which is thought to explain the Fenton processes for COD removal response. In the PFP process, R^2, adjusted R^2, and predicted R^2 were determined as 0.99, 0.97, and 0.93, respectively. In the PEFP process, R^2, adjusted R^2, and predicted R^2 were determined as 0.99, 0.99, and 0.98, respectively. The larger the value of the multivariate correlation coefficient R^2, the better the correlation [13]. R^2 values for PFP and PEFP were close to 1, which indicates that the model has a good adequacy, and the responses obtained using the RSM model agreed well with the experimental data.

Statistically, the difference of adjusted R^2 and predicted R^2 is suggested to be <0.2, while C.V. is suggested to be <10%. As seen from Table 6, the difference of adjusted R^2 and predicted R^2 was smaller than 0.2, and C.V. was smaller than 10% (5.23% for PFP and 3.46% for PEFP). A high adjusted R^2 value indicates that the model terms are quite important.

Table 6. ANOVA results of PFP and PEFP for the COD removal (%) response (quadratic model).

	PFP					PEFP				
Source	**SS**	**DF**	**MS**	**F Value**	***p* Value**	**SS**	**DF**	**MS**	**F Value**	***p* Value**
Model	1.15	9	0.13	116.59	<0.0001	0.94	9	0.10	225.77	<0.0001
X_1-pH	0.99	1	0.99	903.68	<0.0001	0.83	1	0.83	1775.51	<0.0001
X_2-Fe^{2+}/i	0.031	1	0.031	28.41	0.0031	0.063	1	0.063	135.51	<0.0001
X_3-H_2O_2	0.029	1	0.029	26.18	0.0037	4.5×10^{-4}	1	4.5×10^{-4}	0.97	0.3704
X_1X_2	1.6×10^{-3}	1	1.6×10^{-3}	1.45	0.2818	3.6×10^{-3}	1	3.6×10^{-3}	7.74	0.0388
X_1X_3	0.014	1	0.014	13.09	0.0152	2.25×10^{-4}	1	2.25×10^{-4}	0.48	0.5177
X_2X_3	4.9×10^{-3}	1	4.9×10^{-3}	4.45	0.0886	0.011	1	0.011	23.71	0.0046
X_1^2	0.075	1	0.075	68.16	0.0004	2.792×10^{-3}	1	2.792×10^{-3}	6.00	0.0579
X_2^2	2.3×10^{-5}	1	2.308×10^{-5}	0.021	0.8905	0.022	1	0.022	47.69	0.0010
X_3^2	1.869×10^{-3}	1	1.869×10^{-3}	1.70	0.2492	0.021	1	0.021	44.67	0.0011
Residual	5.5×10^{-3}	5	1.1×10^{-3}			2.325×10^{-3}	5	4.650×10^{-4}		
Lack of fit	5.3×10^{-3}	3	1.767×10^{-3}	17.67	0.0540	9.25×10^{-4}	3	3.083×10^{-4}	0.44	0.7491
Pure error	2×10^{-4}	2	1×10^{-4}			1.4×10^{-3}	2	7×10^{-4}		
Cor total	1.16	14				0.95	14			
	PFP					**PEFP**				
	R^2	0.99	Std. Dev.	0.033		R^2	0.99	Std. Dev.	0.022	
	Adj R^2	0.97	Mean	0.63		Adj R^2	0.99	Mean	0.62	
	Pred R^2	0.93	C.V. (%)	5.23		Pred R^2	0.98	C.V. (%)	3.46	
	A.P.	31.11	PRESS	0.085		A.P.	46.57	PRESS	0.018	

The F-value of model was 117 and 226 for PFP and PEFP, respectively, with a very low probability value (<0.0001). This indicates that the model is statistically well-fitted and shows that the model is significant.

Lack of fit is an important factor for evaluating the reliability of the model [13]. The "lack fit *p*-value" of the model for PFP and PEFP was identified to be 0.05 and 0.75, respectively, which implied that there was no significant error in the data.

Adequacy of precision (A.P.) measures the signal to noise ratio. A ratio greater than 4 is desirable. In the study, the A.P. of PFP and PEFP was determined to be 31.11 and 46.57, respectively. Additionally, A.P. was greater than 4 in all processes.

To determine the fitting quality of the model at each point in the design, the PRESS value was used. This value is the sum of the squared differences between the estimated and actual values over all the points [26]. PRESS was obtained as 0.085 and 0.018 in PFP and PEFP, respectively.

A "Prob > F" less than 0.05 shows that the model terms are significant. Values greater than 0.10 indicate that the model terms are not significant. In this case, X_1, X_2, X_3, X_1X_3, X_1^2 are significant model terms for PFP, and X_1, X_2 X_1X_2, X_2X_3, X_2^2, X_3^2 are significant model terms for PEFP.

The significance of the main factors on the COD removal efficiency was: pH > Fe^{2+} concentration > H_2O_2 concentration in the PFP process, and pH > current density > H_2O_2 concentration in the PEFP process.

In conclusion, this model is reliable for optimizing PFP and PEFP parameters to achieve the highest COD removal.

The predicted values of the responses were obtained from the quadratic model. The response equations for the removal efficiency of COD by the PFP are given in Equation (11).

Here, Y_1 is the predicted COD removal efficiency for PFP ($0 < Y_1 \leq 100\%$), X_1, X_2, and X_3 are the pH ($3 \leq X_1 \leq 6$), Fe^{2+} concentration ($2.3\ g/L \leq X_2 \leq 3.83\ g/L$), and hydrogen peroxide concentration ($23\ g/L \leq X_3 \leq 54\ g/L$), respectively.

$$Y_1 = \text{COD Removal Efficiency } (\%) - \text{PFP} = 0.7 - 0.3525X_1 + 0.0625X_2 + 0.06X_3 + 0.02\,X_1X_2 + 0.06\,X_1X_3 - 0.035X_2X_3 - 0.1425X_1^2 - 0.0025X_2^2 + 0.0225X_3^2 \quad (11)$$

In PFP, although pH ($p < 0.05$) is the most important parameter affecting the COD removal efficiency in the ANOVA analysis, the coefficient of the pH parameter had a negative sign ($b_1 = -0.35$). This determines the conclusion that an increase in pH reduces the efficiency of COD removal. Likewise, in Equation (11), it is seen that Fe^{2+} concentration and hydrogen peroxide concentration, which are the main parameters, have a positive coefficient ($b_2 = +0.063$), ($b_3 = +0.06$). Increasing the Fe^{2+} concentration and hydrogen peroxide concentration increased the COD removal efficiency.

The predicted values of the responses were obtained from the quadratic model. The response equations for the removal efficiency of COD by PEFP are given in Equation (12).

$$Y_2 = \text{COD Removal Efficiency } (\%) - \text{PEFP} = 0.72 - 0.32X_1 + 0.088X_2 + 0.0075X_3 + 0.03\,X_1X_2 + 0.0075X_1X_3 + 0.053X_2X_3 - 0.028X_1^2 - 0.078X_2^2 - 0.075X_3^2 \quad (12)$$

Here, Y_2 is the predicted COD removal efficiency for PEFP ($0 < Y_2 \leq 100\%$), X_1, X_2, and X_3 are the pH ($3 \leq X_1 \leq 6$), current density ($24\ A/m^2 \leq X_2 \leq 72\ A/m^2$), and hydrogen peroxide ($23\ g/L \leq X_3 \leq 54\ g/L$), respectively.

In PEFP, although pH ($p < 0.05$) is the most important parameter affecting the COD removal efficiency in the ANOVA analysis, the coefficient of the pH parameter had a negative sign ($b_1 = -0.32$). Increasing the pH decreased the efficiency of COD removal. Likewise, in Equation (12), it is seen that Fe^{2+} concentration and hydrogen peroxide concentration, which are the main parameters, have a positive coefficient ($b_2 = +0.088$), ($b_3 = +0.0075$).

As was mentioned by the researchers [27], if the normality plot of the residuals is close to a straight line, there is no need for a conversion of the response. In this study, the normality plot of residuals was close to a straight line, showing that the response did not need converted (Figure 4a,d).

As is seen in Figure 4b,e, the actual values obtained from the experiment were compatible with the predicted values of the model response for both the PFP and PEFP processes.

Main effects of X_1 (A), X_2 (B), and X_3 (C) parameters for PFP and for PEFP are given in Figure 4c,f. It is seen in Figure 4c,f, that, in PFP and PEFP processes, the main effects of X_2 (B) and X_3 (C) had a limited effect on the obtained quadratic model for the COD response. X_1 (A)-pH was the most effective parameter in all processes.

3.2. Interactive Effects of pH, Fe^{2+} Concentration/Current Density, H_2O_2 Concentration on PFP and PEFP for COD Degradation

After the ANOVA evaluation, 2D graphs were created for the interaction parameters. The interactive effects of pH/Fe^{2+} concentration on PFP and pH/current density on PEFP are given in Figures 5a and 6a, respectively. COD removal efficiency positively affected pH for all Fenton processes because of the effect of occurring hydroxyl radicals on low pH values. Low pH values and a high Fe^{2+} concentration or current density had a positive effect on the high COD removal efficiency.

COD removal efficiency was >80% at the pH of 3 in PFP and PEFP. In PEFP, the pH of the solution was an important factor for both the electrolytic generation of H_2O_2 and in the production of free radicals. In the study, the removal efficiency of COD from textile wastewater by the electrochemical-Fenton process at optimum conditions was 82.1% (COD_i: 1310 mg/L, pH: 3, retention time (R.T.): 40 min, current density (C.D.): 4.76 mA/cm^2) [28]. In another study, the COD degradation efficiency of photo-electro-Fenton at optimum conditions (pH: 3, C.D.: 0.30 A/dm^2, C_{H2O2}: 300 mg/L, electrode distance: 0.75 cm, UV source: 32 W, wave length: 254 nm, R.T.: 4 h) was 97% [12]. Acidic conditions are

most effective in Fenton processes for the degradation of COD, as mentioned by other researchers [11,13,29,30].

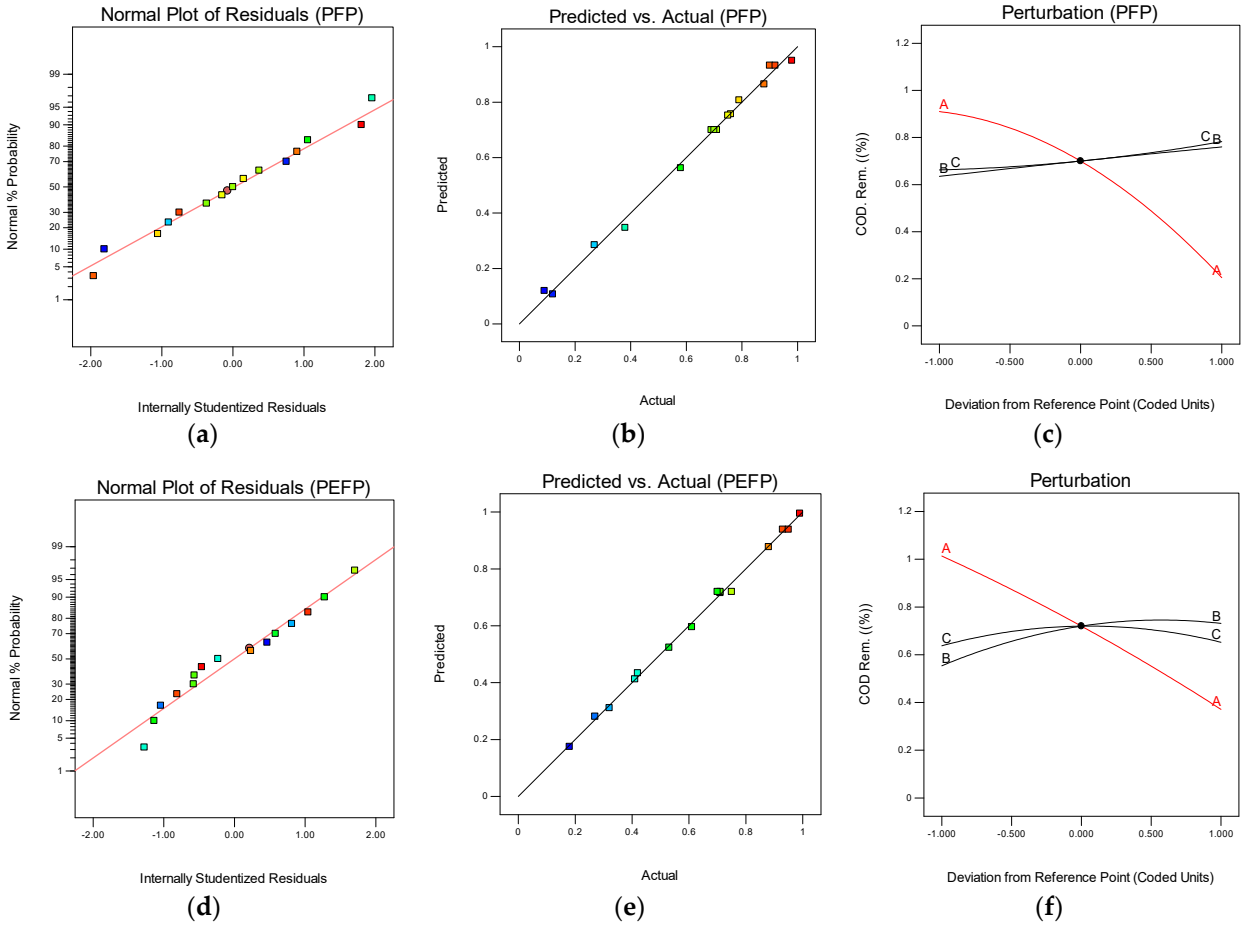

Figure 4. Normality plot of residuals for (**a**) PFP, (**d**) PEFP. Regression plots of the actual and predicted values from the RSM describing COD removal efficiency (**b**) PFP, (**e**) PEFP. Main effects of X_1, X_2, and X_3 parameters: (**c**) PFP, (**f**) PEFP.

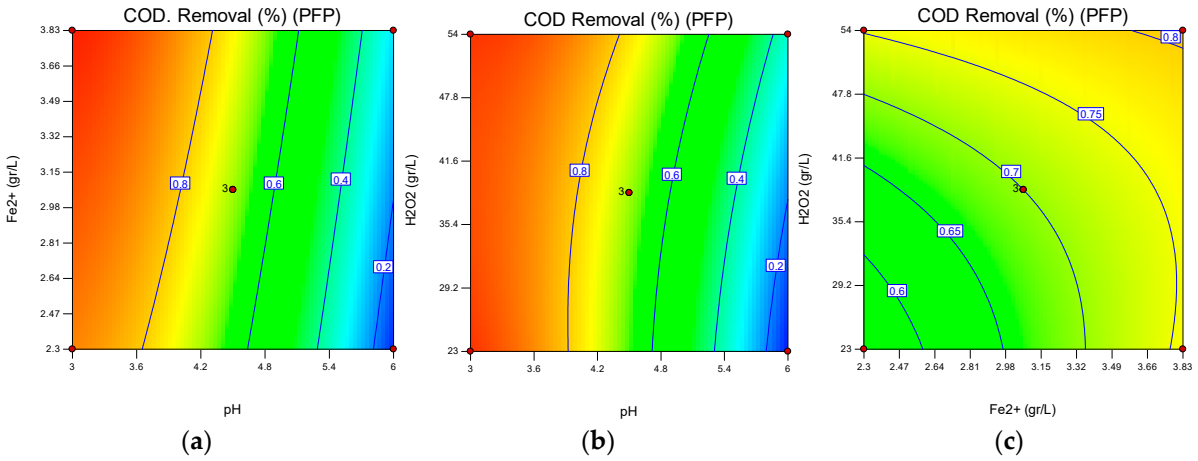

Figure 5. The 2D plots of PFP (**a**) effect of pH/Fe^{2+}, (**b**) effect of pH-H_2O_2 concentration, (**c**) effect of Fe^{2+}-H_2O_2 concentration.

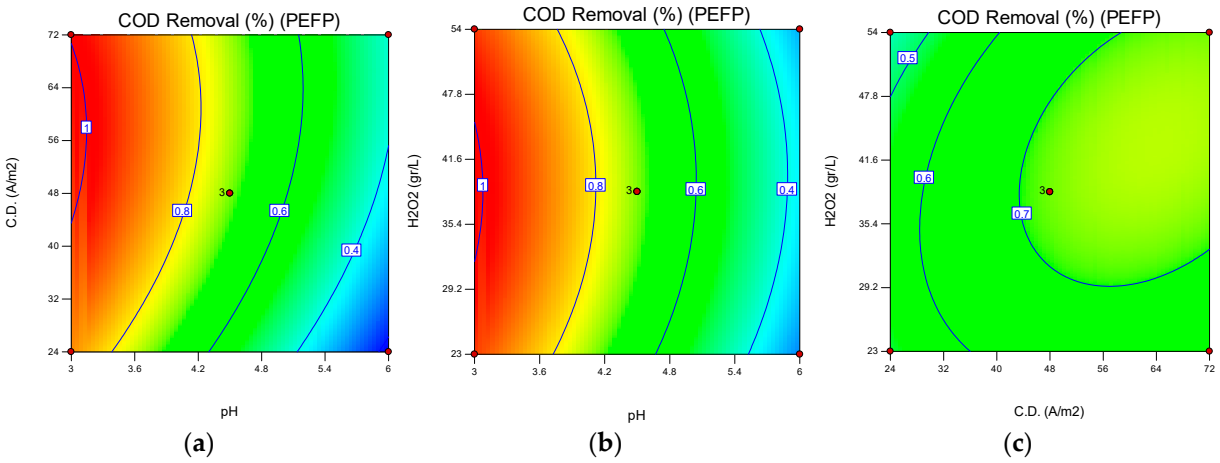

Figure 6. The 2D plots of PEFP (**a**) effect of pH /current density, (**b**) effect of pH-H_2O_2 concentration, (**c**) effect of current density-H_2O_2 concentration.

The effect of pH/H_2O_2 concentration on the COD removal efficiency of PFP and PEFP is given in Figures 5b and 6b, respectively. The pH parameter is more effective than the H_2O_2 concentration in all Fenton processes. Lower pH values provided an effective COD removal efficiency. At a pH > 5, the efficiency of the electro-Fenton process decreased rapidly. This is because the H_2O_2 is unstable in the solution at this pH. When pH > 7, H_2O_2 rapidly decomposes into oxygen and water [31–33]. The 2D plots show the same trend for both Fenton processes. The effect of the H_2O_2 concentration is thought to be limited, as the overdosing of H_2O_2 caused H_2O_2 to self-destruct into water and oxygen [34]. When the excessive H_2O_2 is given to the solution and there is not enough Fe ions in the wastewater, this causes an increase of the cost, and hydroxyl radical production is not provided; it also increases the COD concentration by interfering in the COD analysis [35,36].

The interaction effect of the Fe^{2+} concentration/H_2O_2 concentration on PFP and current density/H_2O_2 concentration on PEFP is given in Figures 5c and 6c, respectively. Statistical results showed that pH, Fe^{2+} concentration, and H_2O_2 concentration parameters are effective in PFP, while pH and current density are effective in PEFP for COD degradation. Ferrous ion is one of the main parameters that influences the photo-Fenton processes because, while the concentration of Fe^{2+} increases, more hydroxyl radicals produce in the solution [20]. With the increase of Fe^{2+} concentration and H_2O_2 concentration, the COD removal efficiency of the PFP increased in the study. An increase of the H_2O_2 concentration occurred for the hydroxyl radical, which increased the removal efficiency of pollutants [37].

In PEFP, increasing the current density increased the COD removal efficiency (Figure 6b). Applying a higher current density increased the efficiency of Fenton chain reactions in a result of the higher electro-regeneration of ferrous ion from ferric ion (Equation (13)). However, after a while, the increase of the current density decreased the COD removal efficiency. When the current density was more, the COD removal efficiency was lower because a high current density causes competitive electrode reactions such as the discharge of oxygen at the anode by reaction (Equation (14)) and the evolution of hydrogen at the cathode by reaction (Equation (15)) [38].

$$Fe^{3+} + e^- \rightarrow Fe^{2+} \quad (13)$$

$$2H_2O \rightarrow 4H^+ + O_2 + 4e^- \quad (14)$$

$$2H^+ + 2e^- \rightarrow H_2 \quad (15)$$

At the same time, when large amounts of H_2O_2 are added to the wastewater, the removal efficiency of Fenton processes decreases due to the hydroxyl radical scavenging effect of H_2O_2 (Equations (16) and (17)) and the recombination of hydroxyl radicals

(Equation (18)) [39]. In the study, in PEFP, increasing the H_2O_2 concentration had a negative effect on the COD removal efficiency.

$$H_2O_2 + {}^{\cdot}OH \rightarrow H_2O + HO_2^{\cdot} \quad (16)$$

$$HO_2^{\cdot} + {}^{\cdot}OH \rightarrow H_2O + O_2 \quad (17)$$

$${}^{\cdot}OH + {}^{\cdot}OH \rightarrow H_2O_2 \quad (18)$$

3.3. Statistical Analysis of Total Operating Cost of PFP and PEFP

The operating cost of PFP consisted of the energy cost of the UV lamp and peristaltic pump, the chemical cost of $FeSO_4$, H_2O_2, NaOH, and H_2SO_4, and the sludge disposal cost.

The operating cost of the PEFP consisted of the energy cost of the UV lamp, peristaltic pump, and DC power supply, the chemical cost of H_2O_2, H_2SO_4, and NaOH, the cost of sludge disposal, and the cost of the Fe electrode.

All the parameters were calculated with the data obtained during the experiment. The calculated values were entered into the software, and as a result of ANOVA, it was seen that the total operating cost was compatible with the quadratic model.

Statistical parameters of the quadratic model for the total operating cost response are given in Table 7. According to the quadratic model, in the PFP process, R^2, adjusted R^2, and predicted R^2 were determined to be 0.99, 0.97, and 0.80, respectively. In the PEFP process, R^2, adjusted R^2, and predicted R^2 were determined to be 0.98, 0.97, and 0.87, respectively. The results of the statistical analysis showed that the R^2 values for PFP and PEFP were close to 1, indicating that the experimental results and statistical values were compatible.

Table 7. ANOVA results of PFP and PEFP for the operating cost (USD/m^3) response (quadratic model).

			PFP					**PEFP**		
Source	**SS**	**DF**	**MS**	**F Value**	***p* Value**	**SS**	**DF**	**MS**	**F Value**	***p* Value**
Model	20.41	9	2.27	46.18	0.0003	1090.12	9	121.12	47.94	0.0003
X_1-pH	2.946×10^{-3}	1	2.946×10^{-3}	0.060	0.8163	14.32	1	14.32	5.67	0.0631
X_2-Fe^{2+}/i	19.43	1	19.43	395.50	<0.0001	969.03	1	969.03	383.58	<0.0001
X_3-H_2O_2	0.048	1	0.048	0.99	0.3662	0.50	1	0.50	0.20	0.6764
X_1X_2	0.030	1	0.030	0.62	0.4670	0.50	1	0.50	0.20	0.6749
X_1X_3	0.061	1	0.061	1.23	0.3170	0.043	1	0.043	0.017	0.9018
X_2X_3	5.565×10^{-4}	1	5.565×10^{-4}	0.011	0.9194	5.05	1	5.05	2.00	0.2166
X_1^2	0.78	1	0.78	15.92	0.0104	63.38	1	63.38	25.09	0.0041
X_2^2	3.5×10^{-5}	1	3.5×10^{-5}	7.127×10^{-4}	0.9797	6.30	1	6.30	2.49	0.1753
X_3^2	0.092	1	0.092	1.88	0.2286	31.41	1	31.41	12.43	0.0168
Residual	0.25	5	0.049			12.63	5	2.53		
Lack of Fit	0.25	3	0.082			9.08	3	3.03	1.70	0.3909
Pure Error	0.000	2	0.000			3.56	2	1.78		
Cor Total	20.66	14				1102.75	14			
			PFP					**PEFP**		
	R^2	0.98	Std. Dev.	0.22		R^2	0.98	Std. Dev.	1.59	
	Adj R^2	0.97	Mean	16.17		Adj R^2	0.97	Mean	25.03	
	Pred R^2	0.80	C.V. (%)	1.37		Pred R^2	0.87	C.V. (%)	6.35	
	A.P.	19.84	PRESS	3.93		A.P.	19.34	PRESS	153.22	

In the model, the adjusted R^2 and predicted R^2 difference was suggested to be <0.2, and CV was <10%. As is seen from Table 7, the adjusted R^2 and predicted R^2 difference was smaller than 0.2, and C.V. was <10% (1.37% for PFP and 6.35% for PEFP).

The F-value of the model for PFP and PEFP was 46 and 48, respectively, with a very low probability value (0.0003 and 0.0003), indicating that the model was statistically well-fitted. It was determined that the developed model is important in estimating the operating cost of the processes.

The "lack fit *p*-value" of the model for PFP and PEFP was identified to be 0.082 and 3.03, respectively, which implied that there was no significant error in the data.

In the study, in PFP and PEFP, A.P. was determined to be 19.84 and 19.34, respectively. Additionally, A.P. was greater than 4 in all processes.

Values of "Prob > F" less than 0.05 show that model terms are significant. Values greater than 0.10 indicate that the model terms are not significant. In this case, X_2 and X_1^2 were significant model terms for PFP, and X_2, X_1^2, X_3^2 were significant model terms for PEFP.

The significance of the main factors for the operating cost was Fe^{2+} concentration > H_2O_2 concentration > pH in the PFP process, and current density > pH > H_2O_2 concentration in the PEFP process.

The predicted values of the responses were obtained from the quadratic model. The response equations for the total operating cost by the PFP and PEFP are given in Equations (13) and (14). Here, Y_3 is the predicted total operating cost for PFP ($0 < Y_3 \leq 100\%$), X_1, X_2, and X_3 are the pH ($3 \leq X_1 \leq 6$), Fe^{2+} concentration (2.3 g/L $\leq X_2 \leq$ 3.83 g/L), and hydrogen peroxide concentration (23 g/L $\leq X_3 \leq$ 54 g/L), respectively.

In PFP, it is seen in Equation (19) that the coefficient of the pH is negative ($b_1 = -0.02$). Increasing the pH decreased the total operating cost. The Fe^{2+} concentration ($b_2 = +1.56$) and H_2O_2 concentration ($b_3 = +0.077$) had positive signs. Increasing the Fe^{2+} concentration ($b_2 = +1.56$) and H_2O_2 concentration ($b_3 = +0.077$) increased the total operating cost.

$$\begin{aligned} Y_3 = \text{Total operating cost } (\%) - \text{PFP} \\ = 15.84 - 0.02X_1 + 1.56X_2 + 0.077X_3 - 0.087\ X_1X_2 - 0.123\ X_1X_3 + 0.012X_2X_3 + 0.46X_1^2 \\ -0.003X_2^2 + 0.16X_3^2 \end{aligned} \quad (19)$$

Here, Y_4 is the predicted total operating cost for PEFP ($0 < Y_2 \leq 100\%$); X_1, X_2, and X_3 are the pH ($3 \leq X_1 \leq 6$), current density (24 A/m^2 $\leq X_2 \leq$ 72 A/m^2), and hydrogen peroxide (23 g/L $\leq X_3 \leq$ 54 g/L), respectively.

In PEFP, it is seen in Equation (20) that the coefficient of the pH and Fe^{2+} concentration was positive ($b_1 = +1.34$, $b_2 = +11.01$), while the H_2O_2 concentration ($b_3 = -0.25$) was negative. Increasing the pH and Fe^{2+} concentration increased the total operating cost. Increasing hydrogen peroxide decreased the total operating cost. The coefficient efficiency of the Fe^{2+} concentration in the equation was quite high ($b_2 = +11.01$).

$$\begin{aligned} Y_4 = \text{Total operating cost } (\%) - \text{PEFP} \\ = 28.10 + 1.34X_1 + 11.01X_2 - 0.25X_3 + 0.35\ X_1X_2 - 0.1X_1X_3 + 1.12X_2X_3 - 4.14X_1^2 \\ +1.31X_2^2 - 2.92X_3^2 \end{aligned} \quad (20)$$

In the study, the normality plot of residuals of the Fenton processes for the response of total operating cost is given in Figure 7a,d.

As is seen from Figure 7b,e, the actual values obtained from the experiments were compatible with the predicted values of the model response for both PFP and PEFP processes for the total operating cost.

The main effects of the X_1 (A), X_2 (B), and X_3 (C) parameters for PFP and for PEFP are given in Figure 7c,f. In the PFP and PEFP processes, X_1 (A) and X_3 (C) had limited effects on the obtained quadratic model.

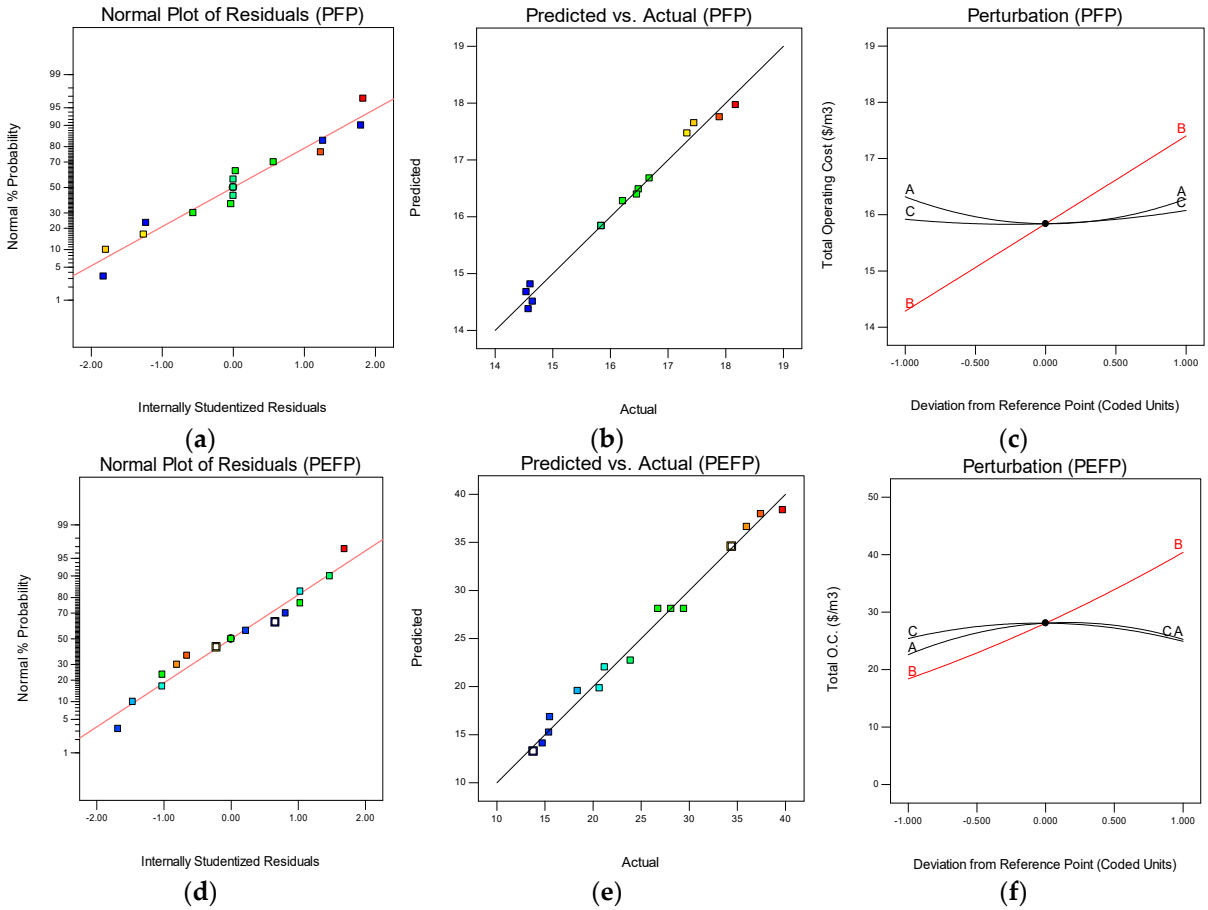

Figure 7. Normality plot of residuals for (**a**) PFP, (**d**) PEFP. Regression plots of the actual and predicted values from the RSM describing total operating cost: (**b**) PFP; (**e**) PEFP. Main effects of X_1, X_2, and X_3 parameters: (**c**) PFP; (**f**) PEFP.

3.4. Optimization of Other Economical Parameters

Optimized techno-economical parameters, equation types, and equations obtained from ANOVA are given in Table 8.

In PFP, at the optimum conditions (pH 3.00, C_{Fe2+} 2.3 g/L, C_{H2O2} 27 g/L), 84% of COD was removed. In the study, 200 mg/L Fe^{2+} concentration, 300 mg/L H_2O_2 concentration and pH 3 were effective for a 93.2% removal of COD from textile wastewaters [8].

The sludge volume (S.V.) of PFP was determined to be 5.97 kg/m^3, and the $FeSO_4$ consumption of the process was 3.61 kg/m^3. Chemical, energy, sludge disposal, and total operating costs were obtained as USD 3.35/m^3, USD 9.52/m^3, USD 1.51/m^3, and USD 14.62/m^3 (USD 4.25/kgCOD), respectively.

At the optimum conditions of PEFP, (pH 3.00, C.D. 27.06 A/m^2, C_{H2O2} g/L 28.16), 90% of COD was removed. Sludge volume was determined to be 3.21 kg/m^3, and electrode and energy consumption of the process were 4.12 kg/m^3 (1.11 kgFe/kgCOD) and 26.90 kWh/m^3 (7.31 kWh/kg COD), respectively. In various electro-Fenton process studies in the literature, it was observed that the energy consumed per kg of COD varied in the range of 1.3–350 kWh without adding UV [29,40–42]. When UV was added to the process, it offered lower energy consumption per kg of COD when compared to the electrochemical Fenton processes without UV. The addition of UV increased the COD removal efficiency.

Electrode, chemical, energy, sludge disposal, and total operating costs of PEFP were obtained as USD 4.08/m^3, USD 0.105/m^3, USD 10.91/m^3, USD 0.61/m^3, and USD 13.79/m^3 (USD 3.73/kgCOD), respectively.

Table 8. Optimized techno-economical parameters of the processes.

PFP					PEFP				
Parameter	**Unit**	**Value**	**Eq.**	**ANOVA Results/Equations**	**Parameter**	**Unit**	**Value**	**Eq.**	**ANOVA Results/Equations**
pH	-	3.00	-	-	pH	-	3.00	-	-
C_{Fe2+}	g/L	2.30	-	-	C.D.	A/m^2	27.06	-	-
C_{H2O2}	g/L	27.00	-	-	C_{H2O2}	g/L	28.16	-	-
E_{COD}	%	84	Q	It is given in Equation (11)	E_{COD}	%	90	Q	It is given in Equation (12)
V_{sludge}	kg/m^3	5.97	Q	$R^2 = 0.99$, $R^2_{Adj} = 0.96$, $R^2_{Pred} = 0.80$ $Y_{sludge} = 6.2 - 0.25 \times X_1 + 2.82 \times X_2 - 0.035 \times X_3 - 0.26 \times X_1X_2 - 0.23 \times X_1X_3 + 0.076 \times X_2X_3 + 2.26 \times {X_1}^2\ 0.12 \times {X_2}^2 + 0.56 \times {X_3}^2$	V_{sludge}	kg/m^3	3.21	Q	$R^2 = 0.93$, $R^2_{Adj} = 0.81$ $Y_{sludge} = 7.2 - 0.06 \times X_1 + 0.74 \times X_2 + 0.24 \times X_3 + 0.22 \times X_1X_2 + 0.06 \times X_1X_3 + 0.053 \times X_2X_3 - 2.3 \times {X_1}^2 - 1.08 \times {X_2}^2 - 0.84 \times {X_3}^2$
C_{FeSO4}	kg/m^3	3.61	L	$R^2 = 1\ R^2_{Adj} = 1$, $R^2_{Pred} = 1$ $Y_{Feso4} = 4.82 - 7.85046e - 016 \times X_1 + 1.204 \times X_2 + 0 \times X_3$	$C_{Fe\ electrode}$	kg/m^3	4.12	Q	$R^2 = 0.98\ R^2_{Adj} = 0.94$, $R^2_{Pred} = 0.75$ $Y_{Fe} = 16.39 + 1.3 \times X_1 + 8.20 \times X_2 - 0.27 \times X_3 - 0.057 \times X_1X_2 - 0.36 \times X_1X_3 + 0.89 \times X_2X_3 - 3.9 \times {X_1}^2 + 1.4 \times {X_2}^2 - 3.15 \times {X_3}^2$
			-		$E_{Cons.}$	kWh/m^3 $kWh/kgCOD$	26.90 7.29	L	$R^2 = 0.96$, $R^2_{Adj} = 0.94$, $R^2_{Pred} = 0.91$ $Y_{energy} = 39.73 + 0.27 \times X_1 + 14.85 \times X_2 - 0.24 \times X_3$
			-		$C_{electrode}$	USD/m^3 $USD/kgCOD$	4.08 1.106	Q	$R^2 = 0.98\ R^2_{Adj} = 0.94$, $R^2_{Pred} = 0.75$ $Y_{Fe} = 16.39 + 1.3 \times X_1 + 8.20 \times X_2 - 0.27 \times X_3 - 0.057 \times X_1X_2 - 0.36 \times X_1X_3 + 0.89 \times X_2X_3 - 3.9 \times {X_1}^2 + 1.4 \times {X_2}^2 - 3.15 \times {X_3}^2$
$C_{Chemical}$	USD/m^3 $USD/kgCOD$	3.35 0.97	L	$R^2 = 0.97$, $R^2_{Adj} = 0.97$, $R^2_{Pred} = 0.95$ $Y_{chemical} = 4.3 + 0.045 \times X_1 + 0.85 \times X_2 + 0.087 \times X_3$	$C_{Chemical}$	USD/m^3 $USD/kgCOD$	0.105 0.028	L	$R^2 = 0.99\ R^2_{Adj} = 0.99$, $R^2_{Pred} = 0.99$ $Y_{chemical} = 0.13 - 0.005 \times X_1 - 0.0014 \times X_2 + 0.048 \times X_3$
C_{Energy}	USD/m^3 $USD/kgCOD$	9.52 2.76	L	-	C_{Energy}	USD/m^3 $USD/kgCOD$	10.91 2.96	L	$R^2 = 0.94\ R^2_{Adj} = 0.92$, $R^2_{Pred} = 0.87$ $Y_{chemical} = 13.23 + 0.061 \times X_1 + 2.68 \times X_2 - 0.053 \times X_3$
C_{sludge}	USD/m^3 $USD/kgCOD$	1.51 0.43	Q	$R^2 = 0.99\ R^2_{Adj} = 0.96$, $R^2_{Pred} = 0.80$ $Y_{slduge} = 1.57 - 0.06 \times X_1 + 0.71 \times X_2 - 0.009 \times X_3 - 0.07 \times X_1X_2 - 0.058 \times X_1X_3 + 0.019 \times X_2X_3 + 0.57 \times {X_1}^2 + 0.030 \times {X_2}^2 + 0.14 \times {X_3}^2$	C_{sludge}	USD/m^3 $USD/kgCOD$	0.61 0.16	Q	$R^2 = 0.93$, Adj $R^2 = 0.81$ $Y_{sludge} = 7.2 - 0.06 \times X_1 + 0.74 \times X_2 + 0.24 \times X_3 + 0.22 \times X_1X_2 + 0.06 \times X_1X_3 + 0.053 \times X_2X_3 - 2.3 \times {X_1}^2 - 1.08 \times {X_2}^2 - 0.84 \times {X_3}^2$
Total O.C.	USD/m^3 $USD/kgCOD$	14.62 4.25	Q	It is given in Equation (19)	Total O.C.	USD/m^3 $USD/kgCOD$	13.79 3.73	Q	It is given in Equation (20)

Q: Quadratic, L: Linear.

The two main parameters that affected the total operating cost of the system are energy consumption and chemical (especially Fenton reagents) costs. The most important parameter among these two parameters is energy cost [43]. In the present study, it was determined that the energy cost of PEFP was the most important parameter that affected the total operating cost of the electro-Fenton processes, as mentioned by other researchers [44,45]. More than half of the total operating cost was due to energy costs [46]. The total operating cost of PEFP was USD 3.73 per removed COD. In a study with an initial COD concentration of 1827 mg/L and at the optimum conditions (pH = 3, current 1 A, $[Fe^{2+}]$ = 0.2 Mm, R.T. = 8 h), 96% of COD was removed from landfill leachate wastewater with an operating cost of USD 8.61–26.72/kgCOD [47]. In the literature, other economic parameters such as sludge disposal, acid, and base chemical cost were not considered. Despite this, the total operating cost of Fenton processes in this study per kg of removed COD is more feasible than other studies in the literature [40,48].

The energy cost (as a unit of USD/m^3 of cost) of the PFP was 15% lower than the PEFP process because of the extra energy requirement of the DC power supply in the PEFP process. The sludge volume of PFP was 85% higher, and the sludge disposal cost of PFP was 2.5 times higher than PEFP. The total operating cost of PFP was 6% higher than PEFP.

It was determined that the chemical cost of the PEFP per kg of removed COD was 34.6 times lower, the sludge disposal cost was 2.7 times lower, and the energy cost was 7% higher than the PFP process. The total operating cost of the PEFP, per kg of removed COD, was 14% lower than PFP. A comparison of the present study and other Fenton studies in the literature is given in Table 9.

Table 9. A comparison of the optimized techno-economical parameters for COD removal efficiency from different wastewaters with various Fenton/electrochemical processes.

Method	Type of Wastewater	Removal Efficiency (%)	Optimum Conditions	Sludge Volume Energy/Chemical Consumption	Total Operating Cost		Literature
					Before a Photovoltaic Solar Panel Integration	After a Photovoltaic Solar Panel Integration	
Photo/Fenton	Denim jean production wastewater	COD: 84% (COD_i: 4100 mg/L) TOC: 61%	pH 3, $C_{Fe}{}^{2+}$: 2.3 g/L, H_2O_2: 27 gr/L, R.T.: 30 min	S.V.: 5.97 kg/m^3 C_{FeSO_4}: 3.61 kg/m^3	USD 4.25/kgCOD USD 14.62/m^3	USD 1.61/kgCOD USD 5.7/m^3	Present Study
Photo/Electrochemical Fenton		COD: 90% (COD_i: 4100 mg/L) TOC: 73%	pH 3, $C_{Fe}{}^{2+}$: 27 A/m^2, H_2O_2: 28 g/L, R.T.: 30 min	S.V.: 3.21 kg/m^3 E.C.:7.29 kWh/kgCOD (26.90 kWh/m^3)	USD 3.73/kgCOD USD 13.79/m^3	USD 1.34/kg COD USD 4.96/m^3	
Solar-Photo-electro-Fenton	Textile wastewater	COD: 83% (COD_i: 545 mg/L)	pH: 4, C.D.: 40 mA/cm^2, $C_{[FeSO_4]}$: 0.3 mM	-	USD 3.45/kgCOD USD 1.56/m^3		[23]
Photo/Fenton	Dairy industry wastewater	COD: 60% (COD_i: 2136 mg/L)	pH 3.5, $C_{[FeSO_4]}$: 198 mg/L, H_2O_2 14,000 mg/L, R.T.: 180 min	-	USD 40.24/kg COD		[29]
Electrochemical Fenton	Nanofiltration concentrate wastewater	COD: 71% (COD_i: 3100 mg/L)	pH: 3, C.D.: 15 mA/cm^2, $C_{[FeSO_4]}$: 560 mg/L, R.T.: 360 min	207 kWh/kgCOD	USD 15.93/kgCOD		[40]
Electro-Fenton	Landfill leachate wastewater	COD: 96% (COD_i: 1827 mg/L)	pH: 3, C.D.: 1A, $C_{[FeSO_4]}$: 0.2 mM, R.T.: 480 min	110–350 kWh/kgCOD	USD 8.61–26.72/kgCOD		[41]
Electro-Fenton	Textile wastewater	COD: 96% (COD_i: 544 mg/L)	pH: 3, C.D.: 0.32 A, $C_{[FeSO_4]}$: 0.53 mM, R.T.: 90 min	1.31 kWh/kgCOD	USD 5.76/kgCOD		[42]
Electro-Fenton	Landfill leachate wastewater	COD: 92.82% (COD_i: 825 mg/L)	pH: 4, U: 5.5 V, H_2O_2/Fe^{2+}: 2.5, R.T.: 50 min, (E:L = 1:2)	3.32 kWh/kgCOD	USD 1.719/kgCOD USD 1.41/m^3		[45]
		COD: 93.35% (COD_i: 792 mg/L)	pH: 4, U: 5.5 V, H_2O_2/Fe^{2+}: 2.5, R.T.: 50 min, (E:L = 1:1)	3.44 kWh/kgCOD	USD 1.722/kgCOD USD 1.36/m^3		
		COD: 91.90% (COD_i: 444 mg/L)	pH: 4, U: 5.5 V, H_2O_2/Fe^{2+}: 2.5, R.T.: 50 min, (E:L = 2:1)	6.24 kWh/kgCOD	USD 1.92/kgCOD USD 0.85/m^3		

3.5. Effect of Solar Panel Integration on Processes

It was reported that electrochemical Fenton processes need to feed the solution with a continuous oxygen source in order to reduce both energy consumption and operating costs by producing H_2O_2 in situ [49]. Another method that minimizes energy consumption and operating costs in electrochemical Fenton processes is the use of solar energy, which

is a renewable energy source. For this reason, a photovoltaic solar panel was integrated directly into the Fenton processes in the study.

The voltage/current from the photovoltaic solar panel was obtained as 35.87 V/0.916 A (Figure 8). Energy consumption was calculated as 32.87 Wh. In the study, the reaction time was obtained as 30 min. Considering that the reactor operated for 30 min, the energy obtained from the photovoltaic solar panel was calculated as 32.87 Wh/0.5 = 16.44 Wh. The energy obtained for liter volume was determined to be 21.91 Wh/lt (16.44 Wh/0.75 mL); 21.91 Wh/lt also equals 21.91 kWh/m^3. Thus, 93% of the energy need of PFP and 81% of PEFP can be supplied from the solar panel.

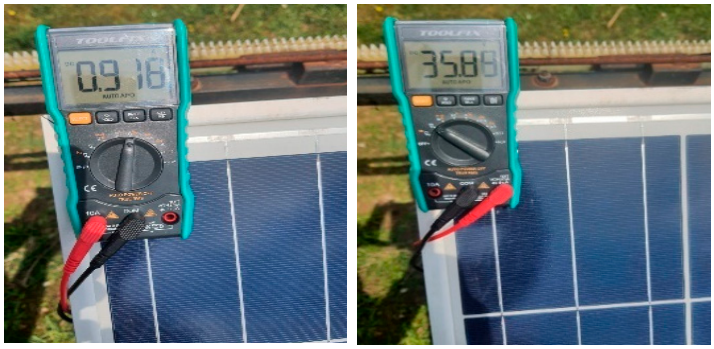

Figure 8. Energy obtained from the photovoltaic solar panel (voltage and amphere).

Generally, 66% and 79% of the total operating costs of the PFP and PEFP processes, respectively, consist of energy costs. With the addition of the photovoltaic solar panel, it caused a 61% and 64% reduction in total operating costs for PFP and PEFP.

The total operating cost was calculated as USD 14.62/m^3 (USD 4.25/kg$COD_{removed}$) without the solar panel and USD 5.7/m^3 (USD 1.61/kg$COD_{removed}$) with the solar panel in PFP. In PEFP, it was calculated as USD 13.79/m^3 (USD 3.73/kg$COD_{removed}$) without the solar panel and USD 4.96/m^3 (USD 1.34/kg$COD_{removed}$) with the solar panel. With the integration of solar energy into electrochemical processes, energy consumption that affects operating cost can be minimized, thus making significant contributions to the environmental sustainability of these processes.

3.6. Biodegradability of Wastewater

The biodegradability of denim processing wastewater after Fenton processes was determined by the following equations (Equations (21) and (22)) [50]:

Carbon oxidation state (COS)

$$COS = 4 - 1.5 * \left(\frac{COD}{TOC_0}\right) \quad (21)$$

Average oxidation state (AOS)

$$AOS = 4 - 1.5 * \left(\frac{COD}{TOC}\right) \quad (22)$$

where TOC is total organic carbon (mg/L) after treatment, and TOC_0 is initial TOC (mg/L) of wastewater. AOS and COS range between +4 for CO_2 and −4 for methane, indicating the most oxidized and most reduced state of carbon [51]. At the optimum conditions, in PFP (pH 3, C_{Fe2+}: 2.3 g/L, H_2O_2: 27 g/L, R.T.: 30 min), 61% of TOC was removed, and in PEFP (pH 3, C_{Fe2+}: 27 A/m^2, H_2O_2: 28 g/L, R.T.: 30 min), 73% of TOC was removed. In PFP, COS and AOS were determined to be 3.64 and 3.09, respectively. In the PFP process, COS and AOS were determined to be 3.77 and 3.17, respectively. High COS values identified that the organic compounds after treatment were comprised mainly of organic acids, and the increase of AOS shows the enhancement of biodegradability [50].

4. Conclusions

In this study, dual criterial optimization, in which the results maximized the COD removal efficiency of denim production wastewater and minimize the operating cost of the PFP and PEFP, was determined by RSM. It was shown that the R^2, R^2_{adj}, and R^2_{pre} values of the COD removal efficiency response and total operating cost response were appropriate for the quadratic model. In the ANOVA analysis of the model, as suggested by the BBD for COD removal and the total operating cost by Fenton processes, statistical parameters of F-value, *p*-value, CV, PRESS, and AP were determined in desirable ranges. Additionally, it was found that BBD could be a reliable statistical model to explain the process/operating parameters and to determine the optimal conditions in terms of COD removal and total operating cost.

As a result of ANOVA, the significance of the main factors for the COD removal efficiency by PFP and PEFP was pH > Fe^{2+} concentration/current density > H_2O_2 concentration. The significance of the main factors for the total operating cost was Fe^{2+} concentration > H_2O_2 concentration > pH in PFP, and it was current density > pH > H_2O_2 concentration in PEFP.

At the optimized conditions based on RSM, in PFP (pH 3, C_{Fe2+}: 2.3 g/L, H_2O_2: 27 g/L, R.T.: 30 min) 85% of COD and 61% of TOC were removed; in PEFP (pH 3, C_{Fe2+}: 27 A/m^2, H_2O_2: 28 g/L, R.T.: 30 min), 90% of COD and 73% of TOC were removed. It was determined that both processes were effective in terms of biodegradability.

Total operating cost was obtained as USD 14.62/m^3 (USD 4.25/kg$COD_{removed}$) and USD 13.79/m^3 (USD 3.73/kg$COD_{removed}$), respectively, in PFP and PEFP. The COD removal efficiency of PFP was 7% lower than PEFP, while the total operating cost of PFP was 6% higher than PEFP (for the cost of USD/m^3).

The sludge volume of PFP was higher in a ratio of 85%, and the sludge disposal cost was approximately 2.5 times higher than PEFP. It was determined that the energy requirement of the PFP process was approximately 15% lower than PEFP because of the extra energy requirement of the DC power supply in PEFP. According to the RSM results, in conditions where the COD removal was maximum and the operating cost was minimum, when the total operating cost was considered, it was determined that the operating cost of PEFP per m^3 of wastewater was 6% cheaper than the PFP, while the total operating cost of PEFP per kg of removed COD was 14% cheaper than PFP.

The addition of the photovoltaic solar panel to the processes resulted in a 61% and 64% reduction in total operating cost for PFP and PEFP, respectively. This study demonstrated the importance of integrating solar energy into UV-assisted Fenton and electrochemical Fenton processes, reducing total operating costs and preferring these processes.

According to all techno-economical evaluations, PEFP is a technique that produces less sludge, consumes less chemicals, offers lower operating costs, and offers more effective COD and TOC removal compared to the PFP process.

Funding: This study did not receive any specific grant from funding agencies in the public, commercial, or not-for-profit sectors.

Data Availability Statement: Contact correspondence author.

Conflicts of Interest: The author has no conflict of interest to declare.

References

1. Moreno-Casillas, H.A.; Cocke, D.L.; Gomes, J.A.G.; Morkovsky, P.; Parga, J.R.; Peterson, E. Electrocoagulation mechanism for COD removal. *Sep. Purif. Technol.* **2007**, *56*, 204–211. [CrossRef]
2. Mousavi, S.; Nazari, S. Applying Response Surface Methodology to Optimize the Fenton Oxidation Process in the Removal of Reactive Red 2. *Pol. J. Environ. Stud.* **2017**, *26*, 765–772. [CrossRef] [PubMed]
3. Dotto, J.; Fagundes-Klen, M.R.; Veit, M.T.; Palacio, S.M.; Bergamasco, R. Performance of different coagulants in the coagulation/flocculation. *J. Clean. Prod.* **2019**, *208*, 656–665. [CrossRef]

4. Bener, S.; Bulca, Ö.; Palas, B.; Tekin, G.; Atalay, S.; Ersöz, G. Electrocoagulation process for the treatment of real textilewastewater: Effect of operative conditions on the organic carbon removal and kinetic study. *Process Saf. Environ. Prot.* **2019**, *129*, 47–54. [CrossRef]
5. Shoukat, R.; Khan, S.J.; Jamal, Y. Hybrid anaerobic-aerobic biological treatment for real textile wastewater. *J. Water Process Eng.* **2019**, *29*, 100804. [CrossRef]
6. Aydıner, C.; Kiril Mert, B.; Can Dogan, E.; Yatmaz, H.C.; Dagli, S.; Aksu, S.; Tilki, Y.M.; Esin Balci, A.Y.G. Novel hybrid treatments of textile wastewater by membrane oxidation reactor: Performance investigations, optimizations and efficiency comparisons. *Sci. Total Environ.* **2019**, *683*, 411–426. [CrossRef]
7. Kuleyin, A.; Gök, A.; Akbal, F. Treatment of textile industry wastewater by electro-Fenton process using graphite electrodes in batch and continuous mode. *J. Environ. Chem. Eng.* **2021**, *9*, 104782. [CrossRef]
8. Deniz, Ç.Ç.; Çifçi, İ. Comparison of kinetics and costs of Fenton and photo-Fenton processes used for the treatment of a textile industry wastewater. *J. Environ. Manag.* **2022**, *304*, 114234.
9. Khan, N.A.; Khan, A.H.; Tiwari, P.; Zubair, M.; Naushad, M. New insights into the integrated application of Fenton-based oxidation processes for the treatment of pharmaceutical wastewater. *J. Water Process Eng.* **2021**, *44*, 102440. [CrossRef]
10. Rezgui, S.; Ghazouani, M.; Bousselmi, L.; Akrout, H. Efficient treatment for tannery wastewater through sequential electro-Fenton and electrocoagulation processes. *J. Environ. Chem. Eng.* **2022**, *10*, 107424. [CrossRef]
11. Can-Güven, E. Advanced treatment of dye manufacturing wastewater by electrocoagulation and electro-Fenton processes: Effect on COD fractions, energy consumption, and sludge analysis. *J. Environ. Manag.* **2021**, *300*, 113784. [CrossRef]
12. Asaithambi, P.; Govindarajan, R.; Yesuf, M.B.; Alemayehun, E. Removal of color, COD and determination of power consumption from landfill leachate wastewater using an electrochemical advanced oxidation processes. *Sep. Purif. Technol.* **2020**, *233*, 115935. [CrossRef]
13. Meng, G.; Jiang, N.; Wang, Y.; Zhang, H.Y.; Tang, Y.; Bai, L.J. Treatment of coking wastewater in a heterogeneous electro-Fenton system: Optimization of treatment parameters, characterization, and removal mechanism. *J. Water Process Eng.* **2022**, *45*, 102482. [CrossRef]
14. Ribeiro, J.P.; Marques, C.C.; Portugal, I.; Nunes, M.I. AOX removal from pulp and paper wastewater by Fenton and photo-Fenton processes: A real case-study. *Energy Rep.* **2020**, *6*, 770–775. [CrossRef]
15. Mirzaei, A.; Chen, Z.; Haghighat, F.; Yerushalmi, L. Removal of pharmaceuticals from water by homo/heterogonous Fenton-type processes—A review. *Chemosphere* **2017**, *174*, 665–688. [CrossRef]
16. Casado, J. Towards industrial implementation of electro-Fenton and derived technologies for wastewater treatment: A review. *J. Environ. Chem. Eng.* **2019**, *7*, 102823. [CrossRef]
17. Exposito, A.J.; Monteagudo, J.M.; Díaz, I.; Dur´an, A. Photo-fenton degradation of a beverage industrial effluent: Intensification with persulfate and the study of radicals. *Chem. Eng. J.* **2016**, *306*, 1203–1211. [CrossRef]
18. Gamarra-Güere, C.D.; Dionisio, D.; Santos, G.O.S.; Lanza, M.R.V.; Motheo, A.J. Application of Fenton, photo-Fenton and electro-Fenton processes for the methylparaben degradation: A comparative study. *J. Environ. Chem. Eng.* **2022**, *10*, 106992. [CrossRef]
19. Moradi, M.; Elahinia, A.; Vasseghian, Y.; Dragoi, E.N.; Omidi, F.; Khaneghah, A.M. A review on pollutants removal by Sono-photo -Fenton processes. *J. Environ. Chem. Eng.* **2020**, *8*, 104330. [CrossRef]
20. Muruganandham, M.; Swaminathan, M. Decolourisation of Reactive Orange 4 by Fenton and photo-Fenton oxidation technology. *Dye. Pigment.* **2004**, *63*, 315–321. [CrossRef]
21. Ting, W.P.; Lu, M.C.; Huang, Y.H. The reactor design and comparison of fenton, electro-fenton and photoelectron-fenton processes for mineralization of benzene sulfonic acid (BSA). *J. Hazard. Mater.* **2008**, *156*, 421–427. [CrossRef] [PubMed]
22. Babuponnusami, A.; Muthukumar, K. Advanced oxidation of phenol: A comparison between Fenton, electro-Fenton, sono-electro-Fenton and photo-electro-Fenton processes. *Chem. Eng. J.* **2012**, *183*, 1–9. [CrossRef]
23. GilPavas, E.; Dobrosz-Gómez, I.; Ángel Gómez-García, M. Optimization of solar-driven photo-electro-Fenton process for the treatment of textile industrial wastewater. *J. Water Process Eng.* **2018**, *24*, 49–55. [CrossRef]
24. APHA (American Public Health Association). *Standard Methods for the Examination of Waste and Wastewater*, 19th ed.; American Public Health Association: Washington, DC, USA, 2005.
25. Aravind, P.; Subramanyan, V.; Ferro, S.; Gopalakrishnan, R. Eco-friendly and facile integrated biological-cum-photo assisted electrooxidation process for degradation of textile wastewater. *Water Res.* **2016**, *93*, 230–241. [CrossRef] [PubMed]
26. Tak, B.; Tak, B.; Kim, Y.; Park, Y.; Yoon, Y.; Min, G. Optimization of color and COD removal from livestock wastewater by electrocoagulation process: Application of Box–Behnken design (BBD). *J. Ind. Eng. Chem.* **2015**, *28*, 307–315. [CrossRef]
27. Jing, L.; Chen, B.; Wen, D.; Zheng, J.; Zhang, B. Pilot-scale treatment of atrazine production wastewater by UV/O_3/ultrasound: Factor effects and system optimization. *J. Environ. Manag.* **2017**, *203*, 182–190. [CrossRef]
28. Ghanbari, F.; Moradi, M. A comparative study of electrocoagulation, electrochemical Fenton, electro-Fenton and peroxi-coagulation for decolorization of real textile wastewater: Electrical energy consumption and biodegradability improvement. *J. Environ. Chem. Eng.* **2015**, *3*, 499–506. [CrossRef]
29. Trigueros, D.E.G.; Braun, L.; Hinterholz, C.L. Environmental and economic feasibility of the treatment of dairy industry wastewater by photo-Fenton and electrocoagulation process: Multicriteria optimization by desirability function. *J. Photochem. Photobiol. A Chem.* **2022**, *427*, 113820. [CrossRef]

30. Wang, Z.; Qiao, H.; Yu, Z.; Yang, X.; Tang, Z.; Zhou, W.; Zhao, H. Source analysis of benzene degradability in floating cathode electro-fenton system based on COD removal ratio. *J. Water Process Eng.* **2022**, *46*, 102568. [CrossRef]
31. Wang, Q.; Lemley, A.T. Kinetic model and optimization of 2,4-D degradation by anodic Fenton treatment. *Environ. Sci. Technol.* **2001**, *35*, 4509–4514. [CrossRef]
32. Shemer, H.; Linden, K.G. Degradation and by-product formation of diazinon in water during UV and UV/H2O2 treatment. *J. Hazard. Mater.* **2006**, *136*, 553–559. [CrossRef]
33. Nidheesh, P.N.; Gandhimathi, R. Trends in electro-Fenton process for water and wastewater treatment: An overview. *Desalination* **2012**, *299*, 1–15. [CrossRef]
34. Mohajeri, S.; Aziz, H.A.; Isa, M.H.; Zahed, M.A.; Adlan, M.N. Statistical optimization of process parameters for landfill leachate treatment using electro-Fenton technique. *J. Hazard Mater.* **2010**, *176*, 749–758. [CrossRef] [PubMed]
35. Jin, L.; Luan, Z.; Yu, L.; Ji, Z. Pretreatment of acrylic fiber manufacturing wastewater by the Fenton process. *Desalination* **2012**, *284*, 62–65.
36. Babuponnusami, A.; Muthukumar, K. A review on Fenton and improvements to the Fenton process for wastewater treatment. *J. Environ. Chem. Eng.* **2014**, *2*, 557–572. [CrossRef]
37. Ting, W.P.; Lu, M.C.; Huang, Y.H. Kinetics of 2,6-dimethylaniline degradation by electro-Fenton process. *J. Hazard. Mater.* **2009**, *161*, 1484–1490. [CrossRef]
38. Zhang, H.; Fei, C.; Zhang, D.; Tang, F. Degradation of 4-nitrophenol in aqueous medium by electro-fenton method. *J. Hazard. Mater.* **2007**, *145*, 227–232. [CrossRef]
39. Welling, C. Fenton's reagent revisited. *Acc. Chem. Res.* **1975**, *8*, 125–131. [CrossRef]
40. Hu, Y.; Lu, Y.; Liu, G.; Luo, H.; Zhang, R.; Cai, X. Effect of the structure of stacked electro-Fenton reactor on treating nanofiltration concentrate of landfill Leachate. *Chemosphere* **2008**, *202*, 191–197. [CrossRef]
41. El Kateb, M.; Trellu, C.; Darwich, A.; Rivallin, M.; Bechelany; Nagarajan, M.S. Electrochemical advanced oxidation processes using novel electrode materials for mineralization and biodegradability enhancement of nanofiltration concentrate of landfill leachates. *Water Res.* **2019**, *162*, 446–455. [CrossRef]
42. Kaur, P.; Sangal, V.; Kushwaha, J.P.K. Parametric study of electro-Fenton treatment for real textile wastewater, disposal study and its cost analysis. *Int. J. Environ. Sci. Technol.* **2019**, *16*, 801–810. [CrossRef]
43. Ismail, S.A.; Ang, W.L.; Mohammad, A.W. Electro-Fenton technology for wastewater treatment: A bibliometric analysis of current research trends, future perspectives and energy consumption analysis. *J. Water Process Eng.* **2021**, *40*, 101952. [CrossRef]
44. Gaied, F.; Louhichi, B.; Jeday, M.R. Tertiary treatment of waste water by electro-fenton process: Economical study. In Proceedings of the 2017 International Conference on Green Energy Conversion Systems (GECS), Hammamet, Tunisia, 23–25 March 2017; pp. 2–5.
45. Li, M.; Zhou, M.; Qin, X. A feasible electro-Fenton treatment of landfill leachate diluted by electro-Fenton effluent: Evaluation of operational parameters, effect of dilution ratio and assessment of treatment cost. *J. Water Process Eng.* **2022**, *47*, 102754. [CrossRef]
46. Chai, Y.; Qin, P.; Zhang, J.; Li, T.; Dai, Z.; Wu, Z. Simultaneous removal of Fe(II) and Mn(II) from acid mine wastewater by electro-Fenton process. *Process Saf. Environ. Prot.* **2020**, *143*, 76–90. [CrossRef]
47. Varank, G.; Yazıcı, S.; Güvenç, K.; Dinçer, D.A. Concentrated leachate treatment by electro-Fenton and electro-persulfate processes using central composite design. *Int. J. Environ. Res.* **2020**, *14*, 439–461. [CrossRef]
48. Tripathy, B.K.; Kumar, M. Sequential coagulation/flocculation and microwavepersulfate processes for landfill leachate treatment: Assessment of bio-toxicity, effect of pretreatment and cost-analysis. *Waste Manag. (Oxford)* **2019**, *85*, 18–29. [CrossRef]
49. Zhang, Z.; Meng, H.; Wang, Y.; Shi, L.M.; Wang, X.; Chai, S. Fabrication of graphene@ graphite-based gas diffusion electrode for improving H_2O_2 generation in Electro- Fenton process. *Electrochim. Acta* **2018**, *260*, 112–120. [CrossRef]
50. GilPavas, E.; Correa-Sanchez, S. Optimization of the heterogeneous electro-Fenton process assisted by scrap zero-valent iron for treating textile wastewater: Assessment of toxicity and biodegradability. *J. Water Process. Eng.* **2019**, *32*, 100924. [CrossRef]
51. Ahmadi, M.; Ghanbari, F.; Madihi-Bidgoli, S. Photoperoxi-coagulation using activated carbon fiber cathode as an efficient method for benzotriazole removal from aqueous solutions: Modelling, optimization and mechanism. *J. Photochem. Photobiol. A* **2016**, *322–323*, 85–94. [CrossRef]